Hexagonally Poled Lithium Niobate: A Two-Dimensional Nonlinear Photonic Crystal

N. G. R. Broderick,* G. W. Ross, H. L. Offerhaus, D. J. Richardson, and D. C. Hanna
Optoelectronics Research Centre, University of Southampton, Southampton, SO17 1BJ, United Kingdom
(Received 27 October 1999)

We report on the fabrication of what we believe is the first example of a two-dimensional (2D) nonlinear photonic crystal [Berger, Phys. Rev. Lett. **81**, 4136 (1998)], where the refractive index is constant but where the 2nd order nonlinear susceptibility is spatially periodic. Such crystals allow for efficient quasi-phase-matched 2nd harmonic generation using multiple reciprocal lattice vectors. External 2nd harmonic conversion efficiencies >60% were measured with picosecond pulses. The fabrication technique is extremely versatile and should allow for the fabrication of a broad range of 2D crystals including quasicrystals.

PACS numbers: 42.70.Qs, 42.65.Ky, 42.70.Mp

A standard technique for achieving phase matching in nonlinear optics is to modulate the nonlinearity periodically in one dimension [1]. The resulting grating can be used to compensate for the wave vector mismatch caused by the differing group velocities of the waves involved in a given nonlinear process. Recently Berger proposed extending the idea of quasi-phase-matching to multiple spatial dimensions in much the same way as conventional linear gratings have been extended to photonic crystals [2]. In such a nonlinear photonic crystal (NPC) there is a periodic spatial variation of a nonlinear susceptibility tensor while the refractive index is constant. Note that in a NPC the typical period is ~ 10 μm for second harmonic generation at 1.5 μm. The simplest type of NPCs are the 1D quasi-phase-matched materials, first proposed by Armstrong *et al.* [1] in which the second order susceptibility undergoes a periodic change of sign. This type of 1D structure has attracted much interest since the successful development of periodically poled lithium niobate (PPLN) based devices. Here we report the experimental realization as a 2D nonlinear periodic structure with hexagonal symmetry in lithium niobate (HeXLN).

One-dimensional quasi-phase-matching is well understood [3] and so we turn immediately to the idea of quasi-phase-matching of second harmonic generation in two dimensions. Second harmonic generation is a three photon process in which two photons with momentum $\hbar k^{\omega}$ are converted into a photon of momentum $\hbar k^{2\omega}$ and if $k^{2\omega} = 2k^{\omega}$ (ideal phase matching) then the momentum is conserved and the interaction is allowed. In general, ideal phase matching is not possible due to dispersion, and different techniques must be used to ensure conservation of momentum. In the quasi-phase-matched case conservation of momentum becomes [2]

$$\mathbf{k}^{2\omega} - 2\mathbf{k}^{\omega} - \mathbf{G}_{n,m} = 0, \qquad n, m \in \mathbb{Z}, \qquad (1)$$

where $\mathbf{G}_{n,m}$ is a reciprocal lattice vector (RLV) of the nonlinear photonic crystal. For each RLV $\mathbf{G}_{n,m}$ and a prescribed $\mathbf{k}^{\omega}$ there is at most a unique angle of propagation for the second harmonic such that Eq. (1) is satisfied. The coupling strength of a phase-matching process using $\mathbf{G}_{n,m}$ is proportional to the corresponding Fourier coefficient in the decomposition of $\chi^{(2)}(\mathbf{r})$. If a particular Fourier coefficient is zero, then no second harmonic generation will be observed in the corresponding direction. For a hexagonal lattice as shown in Fig. 1 the reciprocal lattice is another hexagonal lattice rotated by only 90°. Thus in contrast with the 1D case there are RLVs at numerous angles, each of which allows phase matching in a different direction [given by Eq. (1)]. Note that for a real space lattice period of d the RL has a period of $4\pi/(\sqrt{3}\,d)$ as compared with $2\pi/d$ for a 1D crystal [4], allowing us to compensate for a greater phase mismatch in a 2D geometry than in a 1D geometry with the same spatial period.

In order to demonstrate the idea of a 2D NPC we poled a wafer of lithium niobate with a hexagonal pattern. Figure 1 shows an expanded view of the resulting structure, which was revealed by lightly etching the sample in acid. Each hexagon is a region of domain inverted material—the total inverted area comprises $\sim 30\%$ of the overall sample area. The fabrication procedure was as follows. A thin layer of photoresist was first deposited onto the $-z$ face of a 0.3 mm thick, z-cut wafer of $LiNbO_3$, and then photolithographically patterned with the hexagonal array. The x-y orientation of the hexagonal structure was carefully

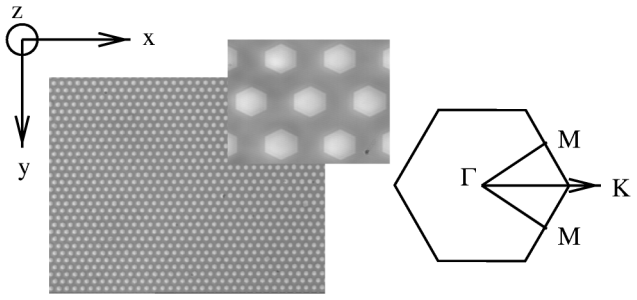

FIG. 1. Picture of the HeXLN crystal and the first Brillouin zone. The period of the crystal is 18.05 μm and is uniform over the whole sample. In our experiments propagation was in the ΓK direction.

aligned to coincide with the crystal's natural preferred domain wall orientation: $LiNbO_3$ itself has triagonal atomic symmetry (crystal class 3*m*) and shows a tendency for domain walls to form parallel to the *y* axis and at $\pm 60°$ as seen in Fig. 1. Poling was accomplished by applying an electric field via liquid electrodes on the $\pm z$ faces at room temperature [5]. Our HeXLN crystal has a period of 18.05 μm, suitable for noncollinear frequency doubling of 1531 nm in the ΓK direction at 150 °C using the reciprocal lattice vector $G_{0,1}$ and its mirror image (an elevated temperature was chosen to eliminate photorefractive effects). The hexagonal pattern was found to be uniform across the sample dimensions of 14 $\times$ 7 mm (*x*-*y*) and was faithfully reproduced on the $+z$ face. Last we polished the $\pm x$ faces of the HeXLN crystal allowing a propagation length of 14 *mm* through the crystal in the ΓK direction (see Fig. 1).

To investigate the properties of the HeXLN crystal we proceeded as follows. The HeXLN crystal was placed in an oven and mounted on a rotation stage which could be rotated by $\pm 15°$ around the *z* axis while still allowing light to enter through the $+x$ face of the crystal. The fundamental pump beam consisted of 4 ps, 300 kW, at 1531 nm pulses obtained from a high power all-fiber chirped pulse amplification (CPA) system [6] operating at a pulse repetition rate of 20 kHz. The output from the CPA system was focused into the HeXLN crystal using a 10 cm focal length lens giving a focal spot diameter of 150 μm and a corresponding peak intensity of ~ 1.8 GW/cm^2. The initial experiments were done at zero angle of incidence corresponding to propagation in the ΓK direction. At low input intensities (~ 0.2 GW/cm^2) the output consisted of multiple output beams of different colors emerging from the crystal at different angles. In particular, two second harmonic beams emerged from the crystal at symmetrical angles of $\pm(1.1 \pm 0.1)°$ from the remaining undeflected fundamental. At slightly wider angles were two green beams (third harmonic of the pump) and at even wider angles were two blue beams (the fourth harmonic). There was also a third green beam copropagating with the fundamental. The output was symmetrical since the input direction corresponded to a symmetry axis of the NPC. As the input power increased, the second harmonic spots remained in the same positions while the green light appeared to be emitted over an almost continuous range of angles rather than the discrete angles observed at low powers. The two second harmonic beams can be understood by referring to the reciprocal lattice of our structure. For propagation in the ΓK direction the closest RLVs are in the ΓM directions, and it is these RLVs that account for the second harmonic light [2].

After filtering out the other wavelengths, the second harmonic (from both beams) was directed onto a power meter, and the efficiency and temperature tuning characteristics for zero input angle were measured. These results are shown in Fig. 2. Note that the maximum external conversion efficiency is greater than 60% and this is constant over a wide range of input powers. Taking into account the Fresnel reflections from the front and rear faces of the crystal this implies a maximum internal conversion efficiency of 82%–41% in each beam. As the second harmonic power was increased, the amount of back conversion increased, which we believe is the main reason for the observed limiting of the conversion efficiency at high powers.

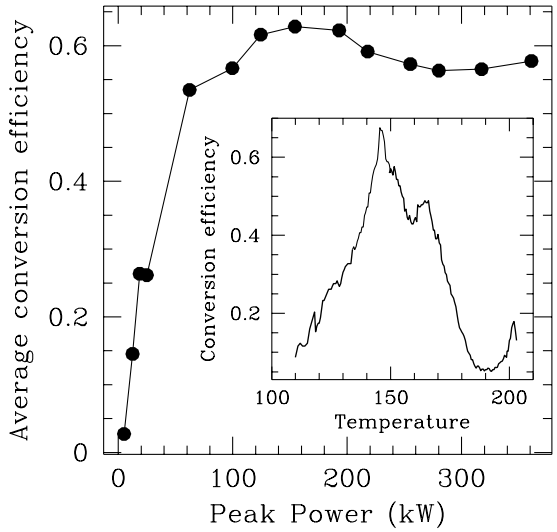

FIG. 2. Second harmonic efficiency of the HeXLN crystal against input peak power. Note that the maximum efficiency is >60% and is limited principally by parametric back conversion. The inset is the temperature tuning of the HeXLN crystal taken at an incident peak power of 300 kW.

Evidence of the strong back conversion can be seen in Fig. 3 which shows the spectrum of the remaining fundamental for both vertically (dashed line), i.e., in the

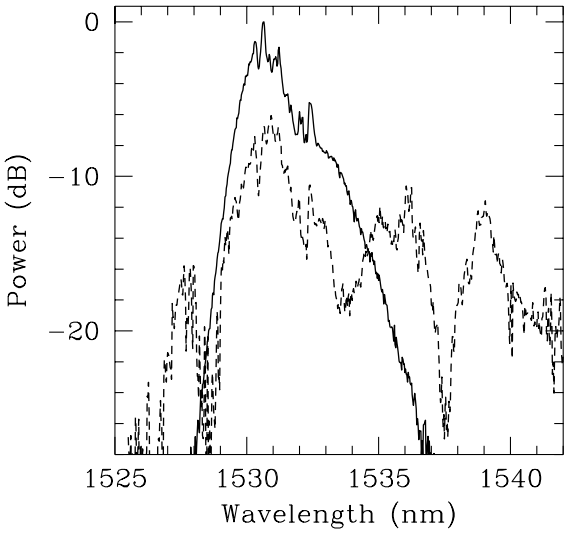

FIG. 3. Output spectra at 1531 nm for both horizontally (solid line) and vertically (dashed line) polarized light. Note the large amount of pump depletion which can clearly be seen along with the back conversion. The incident peak power was 300 kW.

z direction, and horizontally (solid line) polarized input light. As the phase matching works only for vertically polarized light, the horizontally polarized spectrum is identical to that of the input beam and when compared with the other trace (dashed line) shows the effect of pump depletion and back conversion. Note that for vertically polarized light the amount of back-converted light is significant compared to the residual pump which is as expected given the large conversion efficiency. Figure 3 shows ~8 dB (85%) of pump depletion which agrees well with the measured value for the internal efficiency calculated using the time average power measurements.

In the 1D case, for an undepleted pump, the temperature tuning curve is expected to have a $\mathrm{sinc}^2(T)$ shape and to be quite narrow −4.7 °C for a 1D PPLN crystal with the same length and period as the HeXLN crystal used here. However, as can be seen from Fig. 2(inset), the temperature tuning curve (obtained in a similar manner to the power characteristic with a pump power of 300 kW) is much broader with a FWHM of ~25 °C, and it exhibits considerable structure. At present, the reason for the observed increase in bandwidth is not understood and would appear to be due to the added degree of freedom in a two-dimensional crystal for phase matching. We note that Missey *et al.* observed an increase in bandwidth of a noncollinear optically parametric oscillator based on PPLN compared to a collinear optical parametric oscillator using the same crystal [7]. Because of the limitations of the oven, we were not able to raise the temperature above 205 °C and hence could not completely measure the high temperature tail of the temperature tuning curve. Note that temperature tuning is equivalent to wavelength tuning of the pump pulse and hence it should be possible to obtain efficient phase matching over a wide wavelength range at a fixed temperature.

We next measured the angular dependence of the second harmonic beams. As the crystal was rotated, phase matching via different RLVs could be observed. For a particular input angle (which determined the angle between the fundamental and the RLVs) quasi-phase-matched second harmonic generation occurred, via a single RLV, and produced a second harmonic beam at an angle 2θ to the fundamental where θ is given by [2]

$$\frac{\lambda^{2\omega}}{n^{2\omega}} = \frac{2\pi}{|\mathbf{G}|}\sqrt{\left(1 - \frac{n^{\omega}}{n^{2\omega}}\right)^2 + 4\,\frac{n^{\omega}}{n^{2\omega}}\,\sin^2\theta}\,, \qquad (2)$$

where $\lambda^{2\omega}$ is the vacuum wavelength of the second harmonic and $\mathbf{G}$ is the RLV used. These results are shown in Fig. 4 where the solid circles indicate the measured angles of emission for second harmonic while the open squares are the predicted values based on Jundt's coefficients [8]. In the figure, 0° corresponds to propagation in the ΓK direction. Also indicated on the figure are the RLVs used for phase matching, where $[n, m]$ refers to the RLV $\mathbf{G}_{n,m}$. Note

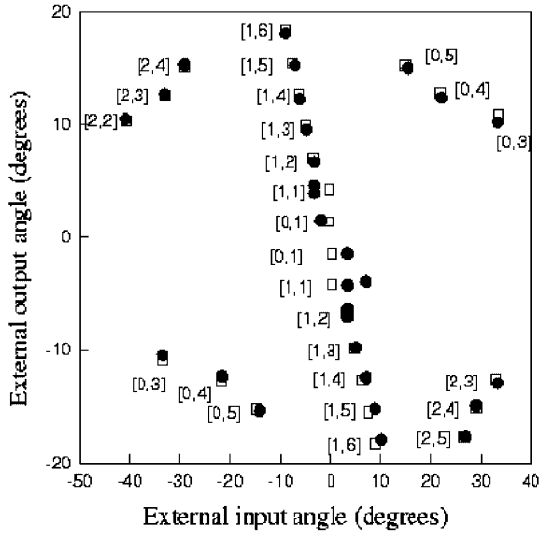

FIG. 4. Graph of the experimental (circles) and theoretical (squares) output angles for the second harmonic as a function of the external input angle, where 0° indicates propagation in the ΓK direction. The maximum internal angle between the fundamental and second harmonic was ~8° (the refractive index of lithium niobate is ~2.2).

that there is good overall agreement between the theoretical and experimental results even for higher order Fourier coefficients which indicates the high quality of the crystal. The inversion symmetry of Fig. 4 results from the hexagonal symmetry of the crystal. To further highlight this symmetry we have labeled the negative output angles with the corresponding positive RLVs. Note that better agreement between the theoretical and experimental values can be achieved by altering the values used for the refractive index of lithium niobate (by less than 2%) and that this effect is largest for the smallest reciprocal lattice vectors which is where the main disagreement lies. However, this does not account for the presence of two observed spots rather than one for some RLVs. At present the reason for these two spots is not understood and is the subject of ongoing work. Pictures of the output of the crystal as a function of the input angle are available elsewhere [9].

For applications where collinear propagation of the fundamental and second harmonic is desirable propagation along the ΓM axis of the HeXLN crystal could be used (since the smallest RLV is in that direction). For the parameters of our crystal collinear second harmonic generation of 1.446 μm in the ΓM direction is expected.

Visually the output of the HeXLN crystal is quite striking with different colors (red, green, and blue) being emitted in different directions [9]. For a range of input angles and low powers distinct green and red spots can been seen each emitted in a different direction, often with the green light emitted at a wider angle than the second harmonic. The presence of the green light implies sum frequency generation between the fundamental and the second harmonic. For this to occur efficiently it must also

be quasi-phase-matched using a RLV of the lattice. In certain regimes (of angle and temperature) simultaneous quasi-phase-matching of both second harmonic generation and sum frequency mixing occurs with as much as 20% of the second harmonic, converted to the green (in multiple beams). For propagation in the ΓK direction the green spot which is collocated with the fundamental is believed to be due to the RLVs $G_{\pm 1,0}$. However, in general we are unable to state which RLVs are responsible for the sum frequency generation due to the uncertainties in the measured values of the angles and the refractive index of lithium niobate.

It should be noted that although lithium niobate preferentially forms domain walls along the y axis and at $\pm 60°$ we are not limited to hexagonal lattices. In fact, essentially any two-dimensional lattice can be fabricated; however, the patterned region of the unit cell will always consist of either a hexagon or a triangle. The shape of the poled region will determine the strength of each of the Fourier coefficients for the RLVs while the lattice structure will determine their position. One can envisage creating more complicated structures such as 2D quasicrystals in which a small poled hexagon is situated at every vertex. Alternatively a HeXLN crystal could be used as an efficient monolithic optical parametric oscillator [2]. Last, we note that NPCs are a specific example of more general nonlinear holograms which would convert a beam profile at one wavelength to an arbitrary profile at a second wavelength [10]. This would be a generalization of the concepts of Imeshev *et al.* who converted a Gaussian profile beam at the fundamental to a square top second harmonic using transversely patterned periodically poled lithium niobate [11].

In conclusion, we have fabricated what we believe to be the first example of a two-dimensional nonlinear photonic crystal in lithium niobate. Because of the periodic structure of the crystal, quasi-phase-matching is obtained for multiple directions of propagation with internal conversion efficiencies of $>80\%$. Such HeXLN crystals could find many applications in optics where simultaneous conversion of multiple wavelengths is required.

The authors gratefully acknowledge useful discussions with Peter Smith and Tanya Monro of the ORC.

*Email address: ngbaoc.soton.ac.uk

[1] J. A. Armstrong *et al.,* Phys. Rev. **127,** 1918 (1962).
[2] V. Berger, Phys. Rev. Lett. **81,** 4136–4139 (1998).
[3] M. M. Fejer *et al.,* IEEE J. Quantum Electron. **28,** 2631–2654 (1992).
[4] Note that in Ref. [1], the period of the reciprocal lattice is stated as $2\pi/d$ where d is the distance between two consecutive planes of nonlinear domains in the crystal, in analogy with the Bragg law, and the lattice period is $2d/\sqrt{3}$ and not d.
[5] M. Yamada, N. Nada, M. Saitoh, and K. Watanabe, Appl. Phys. Lett. **62,** 435–436 (1993).
[6] N. G. R. Broderick, D. J. Richardson, D. Taverner, and M. Ibsen, Opt. Lett. **24,** 566–568 (1999).
[7] M. J. Missey *et al.,* Opt. Lett. **24,** 1227–1229 (1999).
[8] D. H. Jundt, Opt. Lett. **22,** 1553–1555 (1997).
[9] N. G. R. Broderick *et al.,* http://xxx.lanl.gov/abs/physics/9910036.
[10] V. Berger, in *Confined Photon Systems: Fundamentals and Applications,* edited by H. Benisty, J. M. Gerard, R. Houdie, J. Rarity, and C. Weisbuch, Lecture Notes in Physics Vol. 531 (Springer, Heidelberg, 1999), Chap. "Photonic Crystals for Nonlinear Optical Frequency Conversion," pp. 366.
[11] G. Imeshev, M. Proctor, and M. M. Fejer, Opt. Lett. **23,** 673–675 (1998).